

Renormalization persistency of tensor force in nuclei

Naofumi Tsunoda

Department of physics, the University of Tokyo, 7-3-1 Hongo, Bunkyo-ku, Tokyo, Japan

Takaharu Otsuka

*Department of physics and Center for Nuclear Study,
the University of Tokyo, 7-3-1 Hongo, Bunkyo-ku, Tokyo, Japan
National Superconducting Cyclotron Laboratory, Michigan State University, East Lansing, MI, 48824, USA*

Koshiroh Tsukiyama

*Department of physics and Center for Nuclear Study,
the University of Tokyo, 7-3-1 Hongo, Bunkyo-ku, Tokyo, Japan*

Morten Hjorth-Jensen

*Department of Physics and Center of Mathematics for Applications, University of Oslo, N-0316 Oslo, Norway
National Superconducting Cyclotron Laboratory, Michigan State University, East Lansing, MI, 48824, USA*

In this work we analyze the tensor-force component of effective interactions appropriate for nuclear shell-model studies, with particular emphasis on the monopole term of the interactions. Standard nucleon-nucleon (NN) interactions such as AV8' and χN^3LO are tailored to shell-model studies by employing V_{lowk} techniques to handle the short-range repulsion of the NN interactions and by applying many-body perturbation theory to incorporate in-medium effects. We show, via numerical studies of effective interactions for the sd and pf shells, that the tensor-force contribution to the monopole term of the effective interaction is barely changed by these renormalization procedures, resulting in almost the same monopole term as the one of the bare NN interactions. We propose to call this feature *Renormalization Persistency* of the tensor force, as it is a remarkable property of the renormalization and should have many interesting consequences in nuclear systems. For higher multipole terms, this feature is maintained to a somewhat smaller extent. We present general intuitive explanations for the renormalization persistency of the tensor force, as well as analyses of core-polarization terms in perturbation theory. The central force does not exhibit a similar renormalization persistency.

PACS numbers: 21.30.Fe, 21.60.Cs

Keywords: tensor force, effective interaction

I. INTRODUCTION

The nucleon-nucleon (NN) interaction is normally modelled in terms of several components, such as a central force, a spin-orbit force or a tensor force. These mathematical terms accommodate our phenomenological knowledge of the strong interaction, which, when used in a nuclear many-body context is subjected to different renormalization procedures. In the case of nuclear many-body problem, a given renormalization procedure leads to the derivation of an effective interaction, starting from a bare realistic NN interaction. The so-called bare NN interactions exhibit a strong coupling between low-momentum and high-momentum degrees of freedom generated from short-range details of the interaction. By “bare” we mean that the abovementioned strong coupling is left untouched. This coupling is included only implicitly, via various renormalization procedures, in effective interactions used in for example shell-model studies.

As an example of bare NN interactions, the Argonne interactions (AV), which are defined in the form of local operators in the coordinate space, show a strong short-range repulsion [1, 2]. The resultant strong coupling be-

tween low- and high-momentum modes makes the many-body problem highly non-perturbative. On the other hand, in shell-model calculations, the effective interactions used are defined for some specified configuration space (a strongly reduced Hilbert space), normally called the model space. Therefore, the effective interactions for the shell model should be renormalized to include the effect of virtual excitations to configurations not included in the model space.

Although the properties and the effects of the full interaction and various renormalized interactions have been investigated extensively over the years, we feel that there are still important features of the nuclear interaction which deserve some special attention. In particular, we show here via several numerical studies, that the tensor force component of the bare nuclear interaction is left almost unaffected by various renormalization procedures. The monopole component of the tensor force, a component of great interest in studies of the shell evolution (see discussion below) in nuclei toward the drip lines, is barely changed from the bare interaction when the interaction is renormalized. This allows us thereby to extract simple physics interpretations from complicated many-body systems. In this work we label such a lack of renormalization

influence as *Renormalization persistency*, in short just R-Persistency. The R-Persistency is a property exhibited by specific terms of the original nuclear Hamiltonian that are not affected by the renormalization procedure.

On the experimental side, present and future radioactive ion-beam facilities have made it possible to perform experiments that explore nuclei far from the stability line of nuclear chart. Many unexpected and new phenomena have been observed in such experiments carried out at most advanced radioactive ion-beam facilities over the world. One of the most striking results is the breaking of conventional shell structures in neutron-rich nuclei. Such shell evolution, unexpected in the past, is known by now to occur due to a combination of distinct orbit-dependent effect of certain nuclear forces and an unbalanced neutron to proton ratio. In particular, the nuclear tensor force plays a key role here, as proposed by one of the authors [3, 4]. One of the most useful quantities to probe the effect of tensor force is the so-called monopole matrix element. The monopole matrix element of the two-body interaction between two single-particle states labelled j and j' and total two-particle isospin T is defined as

$$V_{jj'}^T = \frac{\sum_J(2J+1)\langle jj'|V|jj'\rangle_{JT}}{\sum_J(2J+1)}, \quad (1)$$

for $j \neq j'$ [18]. Here $\langle \cdot \cdot |V| \cdot \cdot \rangle_{JT}$ denotes the antisymmetrized two-body matrix element coupled to total angular momentum J and total isospin T . The monopole matrix element is crucial for shell evolution, because it affects the effective single particle energy linearly. For instance, if $n_n(j')$ neutrons occupy the single-particle state j' , the effective single particle energy of protons in the state j is given by

$$\Delta\epsilon_p(j) = \frac{1}{2} (V_{jj'}^{T=0} + V_{jj'}^{T=1}) n_n(j'), \quad (2)$$

where $\Delta\epsilon_p(j)$ represents the change of the effective single particle energy of protons in the single-particle state j . When we consider the tensor-force contribution, the monopole matrix elements always have different signs between a pair of spin-orbit partners. For example, the interaction matrix elements $V_{j_>j'}$ and $V_{j_<j'}$ have opposite sign. Here we define $j_>$ and $j_<$ to represent the spin-orbit partners, that is, $j_> = l + 1/2$ and $j_< = l - 1/2$, where l stands for the orbital momentum of a given single-particle state. In this case, the tensor-force changes the spin-orbit splitting between $j_>$ and $j_<$. The shell structure is also altered, in particular if we have a sizable number of neutrons in the single-particle state j' .

In previous studies [3], the tensor-force component in effective interactions for shell-model calculations was, for the sake of simplicity, modelled via the exchange of π and ρ mesons only. To a large extent, this yields results close to the tensor force in realistic NN interactions. In fact, this model describes rather well the experimental data in several mass regions [4]. However, it is far from trivial that the tensor force in effective interactions for the shell-

model can be considered to be given by the exchange of π and ρ mesons only.

The aim of this article is thus to investigate the R-Persistency of the nuclear tensor force and understand the validity of above assumption through theoretical studies, based on realistic NN interactions and microscopic theories for deriving effective interactions, focusing on the effective interaction for the shell model[19].

This work is organized as follows. First we briefly review the theory for constructing an effective interaction in sect. II. In sect. III and sect. V, the R-Persistency of the monopole part of the tensor force from various approaches to the effective interactions will be discussed. In sect. VI we present not only the monopole part but also the two-body matrix elements including multipole part of the various effective interactions and discuss their tensor force components. For the sake of completeness, we include analyses using other NN interactions in sect. VII. The last section contains our conclusions.

II. CONSTRUCTION OF THE EFFECTIVE INTERACTION FOR THE SHELL MODEL

The aim of this section is to give a brief sketch of the theoretical methods we employ in our analyses of the nuclear force. To construct the effective interactions for the nuclear shell model, we use many-body perturbation theory (MBPT). However, as inputs to MBPT, we cannot use bare realistic NN interactions directly, since their high-momentum components make MBPT non-convergent [5]. We integrate out this high-momentum components employing a renormalized interaction defined only in the low-momentum space below a certain sharp cutoff Λ and designed not to change two-body observables like NN scattering data [6]. This recipe defines a cutoff dependent family of interactions, normally labelled as $V_{\text{low}k}(\Lambda)$, which to be more specific, reads

$$V_{\text{low}k}(\Lambda) = P_\Lambda V_{\text{bare}} P_\Lambda + \delta V_{ct}(\Lambda), \quad (3)$$

where P_Λ indicates a projection operator onto the low-momentum space below Λ . The term $\delta V_{ct}(\Lambda)$ represents the correction term coming from the renormalization procedure. In other words, $P_\Lambda V_{\text{bare}} P_\Lambda$ is a simple projection to the low-momentum space, while $\delta V_{ct}(\Lambda)$ has emerged as a result of the renormalization. By construction, $V_{\text{low}k}(\Lambda)$ goes to the original NN interaction in the limit $\Lambda \rightarrow \infty$. A complete renormalization scheme would generate higher-body forces as well, such as three-body and four-body forces, V_{3N} and V_{4N} , respectively. In this work we limit ourselves to two-body (V_{2N}) interactions only. Thus the cutoff dependence of physical quantities can be used to assess the error made by omitting more complicated many-body forces. The term $P_\Lambda V_{\text{bare}} P_\Lambda$ should contain the long-range part of one-pion exchange interaction as a major component.

Next, we proceed to MBPT. The low-momentum interaction $V_{\text{low}k}$ is a good starting point for MBPT be-

cause we can avoid the difficulty caused by the strong short-range repulsion. For a degenerate model space, the effective interaction V_{eff} can be written as

$$V_{\text{eff}} = \hat{Q} - \hat{Q}' \int \hat{Q} + \hat{Q}' \int \hat{Q} \int \hat{Q} - \dots, \quad (4)$$

where $\hat{Q}(E_0)$ is the so-called \hat{Q} -box, defined as

$$\hat{Q}(E_0) \equiv PH_1P + PH_1Q \frac{1}{E_0 - QHQ} QH_1P. \quad (5)$$

Here, the Hamiltonian is divided into an unperturbed part H_0 and an interaction part H_1 , $H = H_0 + H_1$ and the model space is set to be degenerate with respect to the unperturbed Hamiltonian H_0 with energy E_0 . The integration symbols in Eq. (4) represent the inclusion to infinite order of so-called folded diagrams, see Refs. [7, 8] for details. The \hat{Q} -box is given by diagrams which are valence-linked and irreducible, while \hat{Q}' indicates that only diagrams which are of second- or higher-order in terms of the interaction H_1 , are included, see for example Fig. 1.

We can solve Eq. (4) by the following iterative formula

$$V_{\text{eff}}^{(n)} = \hat{Q}(E_0) + \sum_{m=1}^{\infty} \hat{Q}_m(E_0) \{V_{\text{eff}}^{(n-1)}\}^m, \quad (6)$$

where $\hat{Q}_m(E_0) = \frac{1}{m!} \left(\frac{d^m \hat{Q}(\omega)}{d\omega^m} \right)_{\omega=E_0}$. In this work, we take into account diagrams up to second or third order in the interaction H_1 for the calculation of the \hat{Q} -box.

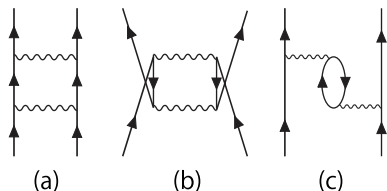


FIG. 1: Examples of diagrams to second-order in the interaction H_1 included in the \hat{Q} -box. The diagrams are referred to as (a) particle-particle ladder, (b) hole-hole ladder and (c) core-polarization, respectively.

By using this two-step method, we can start from an arbitrary bare realistic NN interaction. We calculate effective interactions starting from AV8' [1, 2] and the chiral $\chi\text{N}^3\text{LO}$ interaction [9]. Results using the AV8' interaction are shown in the following sections while our results obtained with the $\chi\text{N}^3\text{LO}$ interaction are shown in sect. VII for the sake of completeness.

Finally, to extract the tensor component from the obtained effective interactions, we employ the spin-tensor decomposition employed in for example Refs. [10–12]

$$\langle abLS|V_p|cdL'S'\rangle_{JT} = (-1)^{J'\hat{p}} \begin{Bmatrix} L & S & J' \\ S' & L' & p \end{Bmatrix} \times \sum_J (-1)^{J\hat{J}} \begin{Bmatrix} L & S & J \\ S' & L' & p \end{Bmatrix} \langle abLS|V|cdL'S'\rangle_{JT}, \quad (7)$$

where $\langle \cdot \cdot LS|V|\cdot \cdot L'S'\rangle_{JT}$ denotes the LS -coupled matrix element of the effective interaction. Here a (as well as bcd) is shorthand for set of quantum numbers (n_a, l_a) , etc. The operator V_p is defined as the scalar product $V_p \equiv U^{(p)} \cdot X^{(p)}$, where $U^{(p)}$ and $X^{(p)}$ are irreducible tensors of rank p , applying to operators in both spin and coordinate space. The tensor component is extracted by setting $p = 2$ in Eq. (7). The terms with hat indicate $\hat{p} = 2p + 1$ and $\hat{J} = 2J + 1$.

III. TENSOR FORCE IN LOW-MOMENTUM INTERACTION $V_{\text{low}k}$

We now present results obtained by the theoretical methods described in the previous section. Figure 2 shows the monopole part of the tensor-force of the renormalized $V_{\text{low}k}$ interaction derived from the Argonne V8' (AV8') potential for the sd -shell and the pf -shell. The cutoff value Λ varies from 1.0 fm^{-1} to 5.0 fm^{-1} . Here, we employ units where $c = \hbar = \hbar^2/m = 1$. The typical value of the cutoff is determined by the best reproduction of the binding energies of ${}^3\text{H}$ and ${}^4\text{He}$. The resulting cutoff value lies around 2.0 fm^{-1} [13]. A too small cutoff Λ (for example 1.0 fm^{-1} in momentum space) cannot resolve the necessary degrees of freedom. Since the Compton length of the pion is approximately 0.7 fm , a cutoff $\Lambda = 1.0 \text{ fm}^{-1}$, which corresponds to 1.0 fm in coordinate space, is too small to resolve the exchange of a pion. Although the resulting renormalized interaction $V_{\text{low}k}$ with $\lambda = 1.0 \text{ fm}^{-1}$ may not contain an appropriate tensor force for shell-model calculations, we include its result in Fig. 2 and subsequent similar figures for the sake of completeness.

We now present the results for the cutoff values $\Lambda = 1.0, 2.1$ and 5.0 fm^{-1} in Fig. 2. The matrix elements are calculated using a harmonic oscillator basis with $\hbar\omega = 14$ and 11 MeV for the sd -shell and the pf -shell, respectively. Except for a very low (and thereby unreasonable) cutoff value $\Lambda = 1.0 \text{ fm}^{-1}$, one finds, both in the sd -shell and the pf -shell, that the monopole part of the tensor force of $V_{\text{low}k}$ has almost no cutoff dependence, and has almost the same strength as that of the original NN interaction. Thus, within the usual values of the cutoff, we can see that the monopole part of the tensor force fulfills the R-Persistence almost perfectly with respect to the renormalization of the short-range part of the NN interaction.

We look now into the robustness and the generality of the features discussed above. For this purpose, we consider the relative motion of two interacting nucleons. The orbital angular momentum of the relative motion can be $L=0$ (S), 1 (P), 2 (D), etc. If the tensor force is acting between two states, there is no coupling between two S states, because the relative coordinate operator in the tensor force is of rank 2. The S -to- S coupling is thus zero. This results in strongly suppressed contributions to the tensor force from the short-range part of the relative-

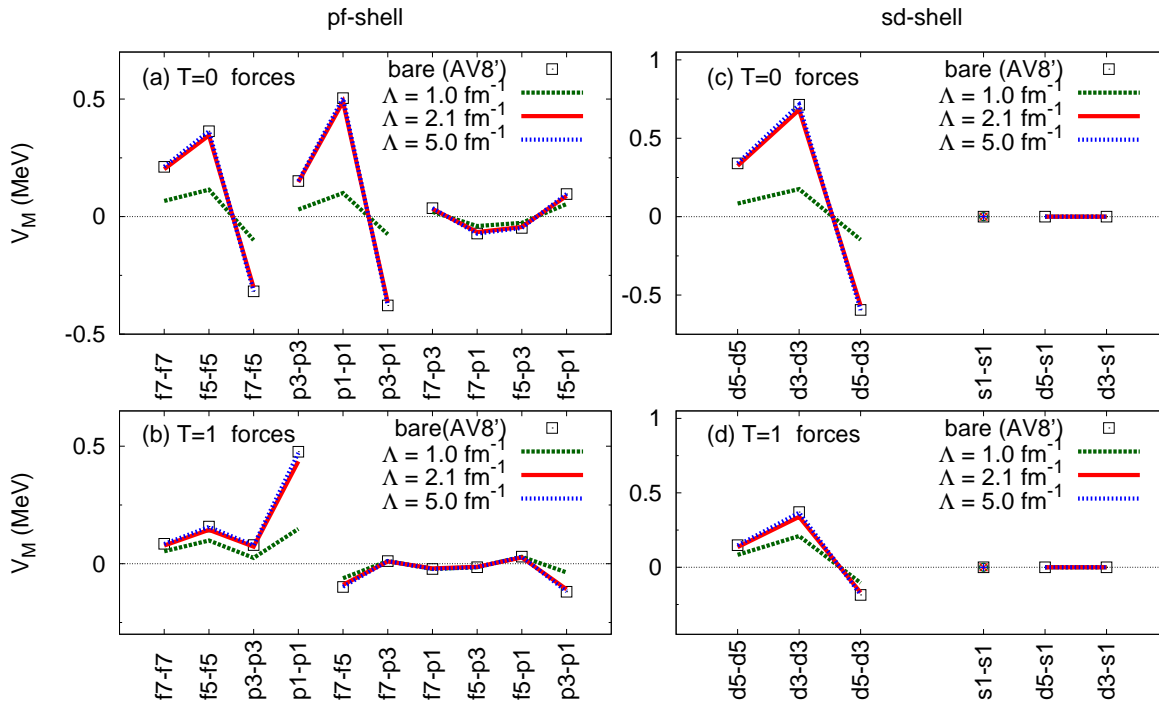


FIG. 2: (color online.) Tensor-force monopole component of low-momentum interaction $V_{\text{low}k}$ as function of the cutoff parameter Λ for (a) $T = 0$ forces in pf -shell, (b) $T = 1$ forces in pf -shell, (c) $T = 0$ forces in sd -shell and (d) $T = 1$ forces in sd -shell. The cutoff parameter Λ of $V_{\text{low}k}$ varies from 1.0 fm^{-1} to 5.0 fm^{-1} .

motion wave function, since a good fraction of the short-range repulsion stems from S waves. Partial waves higher than S waves carry also a centrifugal barrier component which results in smaller short-range contribution to the tensor force relative to S waves. Thus, changes of the potential at short distances do not affect matrix elements of the tensor force for low momentum states. This seems to be the basic reason why the tensor force remains almost the same throughout the renormalization procedure. In other words, there is a sound reason to expect the R-Persistence for the tensor force regarding the treatment of the short-range correlation. On the other hand, the present argument may not be applied to other parts of the nuclear force such as the central force.

The second term δV of Eq. (3) arises for a low-momentum space as a result of the renormalization. It includes for example the central-force component at intermediate inter-nucleon distances, and may affect, in principle, the tensor force as well. The first term, $P_{\Lambda} V_{\text{bare}} P_{\Lambda}$, is exactly equal to the bare tensor force in the limit of $\Lambda \rightarrow \infty$ by definition. In this limit δV is zero. Since matrix elements of the tensor force, particularly for low-momentum states, are not affected much by the short-range modification, the tensor-force-component effect of the first term of Eq. (3) remains the same to a good extent even with finite Λ values, unless it becomes extremely small. The fact that the R-Persistence is almost

perfectly fulfilled in numerical calculations (as we can see in Fig. 2) implies therefore that the second term δV results in small contributions to the tensor force, or does not change longer-range part of the tensor force. The origin of weak tensor force component in δV can be understood by the arguments presented in sect. V, based on the close relation between the the $V_{\text{low}k}$ renormalization process and the MBPT terms representing longer-range corrections, as discussed in [6, 14] as well. We shall come back to this point in sect. V.

IV. RENORMALIZATION OF THE CENTRAL FORCE

Contrary to the tensor force, it can be seen from our numerical studies that the central force does not fulfill the R-Persistence, and is indeed affected strongly by the renormalization procedure due to the short-range part of the NN interaction. This is reflected in a much stronger cutoff dependence as well. The central-force monopole of δV in Eq. (3) is thus not small.

Figure 3 shows the monopole part of the central force of the bare AV8' potential obtained by the decomposition of Eq. (7). In this figure we show also the corresponding central-force monopole component using the $V_{\text{low}k}$ renormalized interaction originating from the AV8' po-

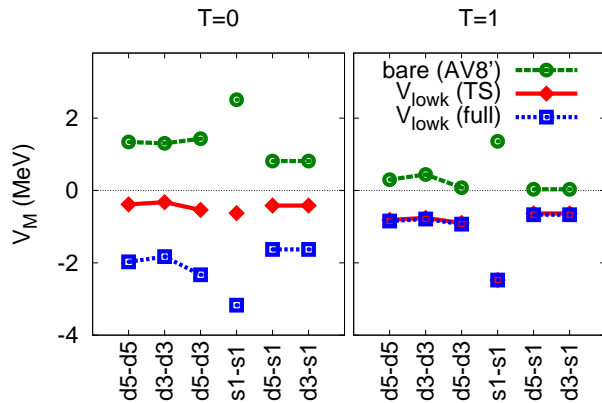


FIG. 3: (color online.) Central-force component of the monopole term of the bare AV8', $V_{\text{low}k}$ (TS) and $V_{\text{low}k}$ (full) in sd -shell, see text for further details and discussions. The central-force component is obtained using the decomposition of Eq. (7). The effect of the renormalization on the short-range tensor force is shown. The cutoff value is chosen as $\Lambda = 2.1 \text{ fm}^{-1}$.

tential, labelled by “full”. We show also results where the tensor force has been subtracted from the bare NN interaction in the renormalization procedure, labelled by “TS” in the figure. What we can see in Fig. 3 is the effect of the renormalization due to the short-range part of the bare realistic NN interaction. The difference between “bare AV8'” and “ $V_{\text{low}k}$ (TS)” lies mainly in the renormalization due to the short-range part of the central force, as the tensor force is subtracted in “ $V_{\text{low}k}$ (TS)”. On the other hand, the difference between “ $V_{\text{low}k}$ (TS)” and “ $V_{\text{low}k}$ (full)” comes solely from the renormalization due to the short-range part of tensor force.

In the $T = 0$ channel, the effect of the renormalization procedure on the short-range part of tensor force is comparable to that of the central force, while in the $T = 1$ channel this effect is almost negligible. This is a quite remarkable feature. Let us discuss this feature in some detail by considering the Schrödinger equation for the deuteron. The deuteron has isospin $T = 0$, spin $S = 1$, orbital momentum $L = 0$ (S -wave) and total angular momentum $J = 1$. There is a small admixture of D -waves as well, leading to the following coupled differential equations for the deuteron

$$\begin{aligned}
 -\frac{\hbar^2}{M} \frac{d^2 u(r)}{dr^2} + V_C u(r) + \sqrt{8} V_T w(r) &= E_d u(r), \\
 -\frac{\hbar^2}{M} \frac{d^2 w(r)}{dr^2} + \left(\frac{6\hbar^2}{Mr^2} + V_C - 2V_T - 3V_{LS} \right) w(r) \\
 + \sqrt{8} V_T u(r) &= E_d w(r),
 \end{aligned} \tag{8}$$

where $u(r)$ and $w(r)$ are the radial wavefunctions of the S -wave and the D -wave, respectively. The potentials V_C , V_{LS} and V_T are the central, spin-orbit and tensor forces, respectively. Knowing the solution of Eq. (8), we can integrate out the D -wave degrees of freedom and

obtain the following effective central force

$$\begin{aligned}
 V_{\text{eff}}(r; {}^3S_1) &= V_C(r; {}^3S_1) + \Delta V_{\text{eff}}(r; {}^3S_1), \\
 \Delta V_{\text{eff}}(r; {}^3S_1) &\equiv \sqrt{8} V_T(r) \frac{w(r)}{u(r)}.
 \end{aligned} \tag{9}$$

The effective central force ΔV_{eff} is comparable to V_C in strength and it makes the ${}^3S_1 - {}^3S_1$, ${}^3S_1 - {}^3D_1$, ${}^3D_1 - {}^3D_1$ coupled channel the most attractive one [15, 16]. This effective central force makes the deuteron bound to the S wave. We can regard this equation as a special case of Eq. (3). The effective central force comes from a second-order effect due to tensor force, since both the initial and the final state have orbital angular momentum 0. As a consequence, the effective interaction for the $T = 0$ channel is enhanced by the effect of renormalization due to the short-range part of the tensor force, while it is not the case in $T = 1$ channel. It reflects the property of the deuteron, which is the only bound two-nucleon system. A similar mechanism may cause the strong cutoff dependence of the $V_{\text{low}k}$ interaction seen in the $T = 0$ channel.

V. TENSOR FORCE IN EFFECTIVE INTERACTION FOR THE SHELL MODEL

We discuss here the tensor-force component in effective interactions for the shell model, using the decomposition of Eq. (7). We have calculated effective interactions for the shell model ($V_{\text{eff}}^{\text{SM}}$) using many-body perturbation theory (MBPT) by considering the \hat{Q} -box up to second and third order with folded diagram included as well, starting from a renormalized $V_{\text{low}k}$ interaction. The cutoff value used in the $V_{\text{low}k}$ calculation is set to $\Lambda = 2.1 \text{ fm}^{-1}$ [13]. The model space (P -space) is chosen to be the full sd -shell or the full pf -shell. In the construction of the $V_{\text{low}k}$ interaction, we renormalized the strong short-range repulsion of the NN interaction, and in MBPT we include further effects of truncations of the model space. The \hat{Q} -box is calculated by considering valence-linked and connected diagrams with unperturbed single particle energies of the harmonic oscillator. The oscillator energy $\hbar\omega$ is set to be 14 MeV and 11 MeV for the sd -shell and the pf -shell effective interactions, respectively. Degenerate perturbation theory is employed in constructing the effective interactions.

Since the Q -space is defined as the complement of the P -space, intermediate states arising in each diagram should be taken up to infinitely high oscillator shells. In our case, using a low-momentum interaction $V_{\text{low}k}$ with $\Lambda = 2.1 \text{ fm}^{-1}$, full convergence of the monopole part of V_{eff} is obtained with approximately 8–10 $\hbar\omega$ excitations in each diagram which makes up the \hat{Q} -box.

Figure 4 shows the monopole part of the tensor force of $V_{\text{eff}}^{\text{SM}}$ defined for the sd -shell or the pf -shell. As a general trend, one can see again that the monopole part of the tensor force of $V_{\text{eff}}^{\text{SM}}$ fulfills our R-Persistence hypothesis to a good extent both in the sd -shell and in the

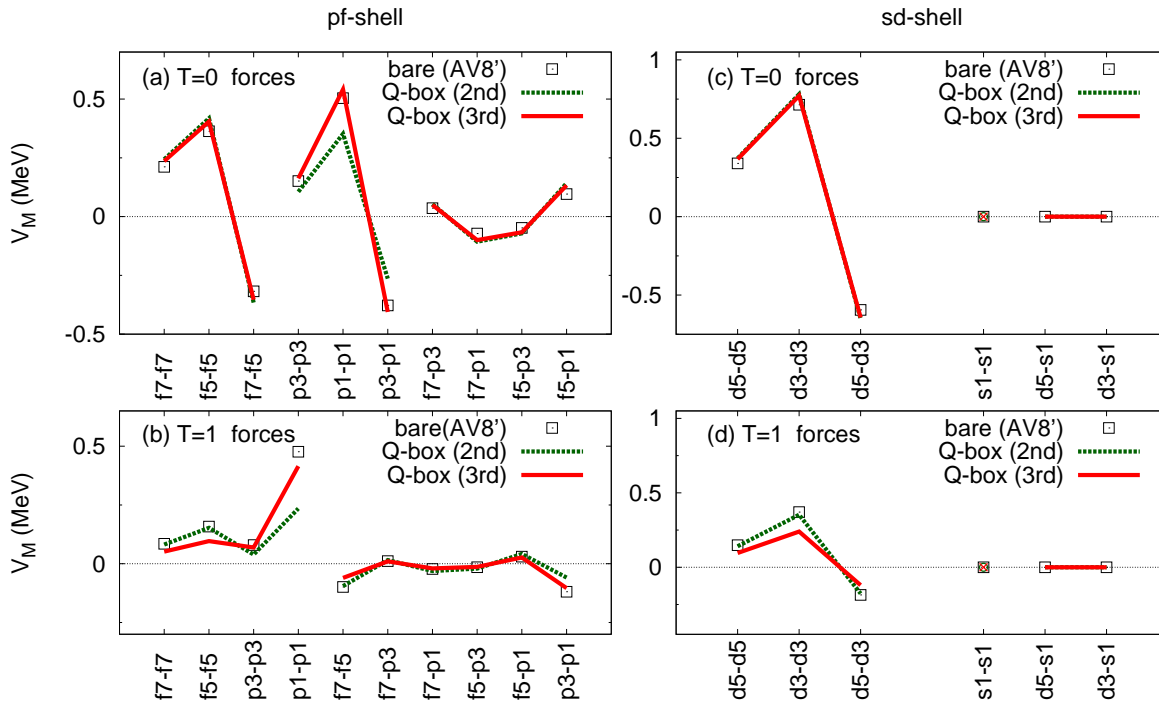


FIG. 4: (color online.) The tensor force monopole component of the effective interaction for the shell model obtained by the \hat{Q} -box expansion to second and third order in the interaction, starting from $V_{lowk}(\Lambda = 2.1 \text{ fm}^{-1})$. The tensor-force component is obtained using the decomposition of Eq. (7) (a) $T = 0$ forces in *pf*-shell, (b) $T = 1$ forces in *pf*-shell, (c) $T = 0$ forces in *sd*-shell and (d) $T = 1$ forces in *sd*-shell.

pf-shell. Since the first order \hat{Q} -box is just the V_{lowk} interaction, the results mean that the monopole part of the tensor force is dominated by the first-order term in the \hat{Q} -box and the contributions from second or higher-order terms are remarkably small. These results can be understood by considering the specific angular momentum structure of the tensor force, which is a scalar product of two rank 2 tensors in spin and coordinate spaces. In a perturbative correction to second or higher-order, such a complicated structure is smeared out and the resultant interaction consists mainly of a central force contribution. Therefore, as for the tensor-force component in the monopole interaction, it is the first-order contribution which is the dominant one.

To elucidate why higher-order terms in many-body perturbation theory are small, we consider as an example a contribution from second order in the interaction, by far the largest higher-order term.

The Hamiltonian causing the present second-order perturbation can be written as

$$H_1 = \sum_{p=0,1,2} w_p (U^{(p)} \cdot X^{(p)}), \quad (10)$$

where w_p stands for strength coefficient, $U^{(p)}$ and $X^{(p)}$ are operators of rank p in spin and coordinate spaces, respectively. The second-order perturbation for state ϕ

is then written as

$$\eta(\phi) = - \sum_j \frac{\langle \phi | H_1 | \psi_j \rangle \langle \psi_j | H_1 | \phi \rangle}{\Delta E_j}, \quad (11)$$

where ψ_j implies an intermediate state with energy denominator ΔE_j . Here, the summation over the intermediate states ψ_j 's is taken. As far as ψ_j varies in this summation, within a fixed configuration with respect to harmonic-oscillator (HO) shells, ΔE_j remains constant, because of the degenerate single-particle energies in a given HO shell, as mentioned earlier (although the usage of non-degenerate perturbation theory yields only small changes). Such a configuration in the HO shell is denoted by S . As ΔE_j is a constant within a fixed S , it is expressed by ΔE_S . Note that S corresponds to a part of the Q -space, while ϕ is in the P -space. $\eta(\phi)$ can be decomposed into contributions from individual S 's as,

$$\eta(\phi) = - \sum_S \frac{\zeta(\phi, S)}{\Delta E_S}, \quad (12)$$

where

$$\zeta(\phi, S) = \sum_{j \in S} \langle \phi | H_1 | \psi_j \rangle \langle \psi_j | H_1 | \phi \rangle. \quad (13)$$

For a given S , all ψ_j s are taken, and the summation can be replaced by closure as

$$\zeta(\phi, S) = \langle \phi | \{H_1 H_1\}_S | \phi \rangle, \quad (14)$$

where the parentheses $\{\}_S$ are introduced to indicate that the second H_1 changes ϕ to an S -configuration state

in the Q -space and the first H_1 moves it back to ϕ in the P -space. In other words, $H_1 H_1$ in this equation cannot be a simple product, but a certain contraction is needed as we shall show soon.

By utilizing Eq. (10), we obtain

$$\begin{aligned} \{H_1 H_1\}_S &= \sum_{p_1, p_2} w_{p_1} w_{p_2} \{ (U^{(p_1)} \cdot X^{(p_1)}) (U^{(p_2)} \cdot X^{(p_2)}) \}_S \\ &= \sum_{k=0,1,2} (2k+1) \left(\sum_{p_1, p_2} w_{p_1} w_{p_2} \begin{Bmatrix} p_1 & p_2 & k \\ p_1 & p_2 & k \\ 0 & 0 & 0 \end{Bmatrix} \{ [[U^{(p_1)} \times U^{(p_2)}]^{(k)} \times [X^{(p_1)} \times X^{(p_2)}]^{(k)}]^{(0)} \}_S \right), \quad (15) \end{aligned}$$

where the terms in curly brackets are $9j$ symbols and k implies the recoupling rank. The operator $\{ [U^{(p_1)} \times U^{(p_2)}]^{(k)} \}_S$ acts in the P -space as rank- k two-body operator in spin space, while $\{ [X^{(p_1)} \times X^{(p_2)}]^{(k)} \}_S$ as rank- k two-body operator in coordinate space. Because the contraction due to the elimination of the Q -space does not affect the angular momentum properties, the variable $k = 0, 1, 2$ represents induced central, spin-orbit and tensor forces in the P -space, respectively.

Since we are mainly interested in the tensor component, we focus on the case of $k = 2$, with the obvious restriction $p_1 + p_2 \geq 2$. Since the above $9j$ symbols is proportional to $1/\sqrt{(2p_1+1)(2p_2+1)}$, it is easy to convince oneself that the central force component receives the largest contribution from the $9j$ symbol. Furthermore, for our analysis it is important to keep in mind that the expectation value of the central component is the largest in absolute value, the tensor component the second largest and the spin-orbit term gives rise to the smallest value to the renormalized V_{lowk} interaction.

From these considerations, for $k = 2$, the largest contribution comes from the combination $p_1 = 0, p_2 = 2$ or $p_1 = 2, p_2 = 0$ in Eq. (10), *i.e.*, central-tensor or tensor-central combination. Let us now discuss this case. We assume without loss of generality that the tensor component of H_1 acts on the ket state of the matrix element being considered. While the central component of H_1 acts afterward on this state, we can also consider that this central force acts to the left on the bra state. We then take the overlap between these two states: one by the tensor on the ket side, and the other by the central on the bra side. These two states are sum-rule states for the two forces, within the S -configuration space. As the

central force and the tensor force are very different in nature, such sum-rule states are very different from each other in general, leading to a very small overlap. This is the main reason why the combination of the central force and the tensor force produces small contributions. The overlap can be even smaller if the bra and ket states are equal due to enhanced orthogonality.

This argument does not hold in the case that the tensor component of H_1 acts twice in the second-order perturbation. However, due to the angular momentum coupling, the product of two tensor forces ($p_1 = p_2 = 2$ in Eq. (10)) yield small contributions to $k = 2$ terms of Eq. (10). For higher orders, other tensor-force components may show up, but there is no mechanism to enhance their contributions.

The small contribution of the tensor force in MBPT can be viewed to be reasonable also under the following intuitive picture: after multiple actions of the forces, the spin dependence is smeared out, and only the distance between two interacting nucleons becomes the primary factor to the whole processes. This results in the dominance of the induced effective interaction by the central components and yields only a minor change in the tensor component.

It is instructive to study in more detail the contributions to second-order in perturbation theory. To do so, we single out the by far largest second-order term, namely the so-called core-polarization term, depicted as diagram (c) in Fig. 1. For the core-polarization diagram we can show that the contribution to tensor force vanishes by simple angular momentum algebra arguments. The contribution to a specific core-polarization matrix element can then be written as

$$\begin{aligned}
\langle am_a b m_b | V_T^{\text{cp-eff}} | c m_c d m_d \rangle &= \sum_{p, m_p, h, m_h} \langle a m_a p m_p | V_C | c m_c h m_h \rangle \langle h m_h b m_b | V_T | p m_p d m_d \rangle / \Delta E \\
&= \sum_{n_p, l_p, n_h, l_h} \left(\sum_{j_p, m_p, j_h, m_h} \langle a m_a p m_p | V_C | c m_c h m_h \rangle \langle h m_h b m_b | V_T | p m_p d m_d \rangle \right) / \Delta E_S \\
&= \sum_{n_p, l_p, n_h, l_h} \left(\sum_{m_{l_p}, m_{s_p}, m_{l_h}, m_{s_h}} \langle a m_a n_p l_p m_{l_p} m_{s_p} | V_C | c m_c n_h l_h m_{l_h} m_{s_h} \rangle \right. \\
&\quad \left. \times \langle n_h l_h m_{l_h} m_{s_h} b m_b | V_T | n_p l_p m_{l_p} m_{s_p} d m_d \rangle \right) / \Delta E_S. \tag{16}
\end{aligned}$$

where $V_T^{\text{cp-eff}}$ is the induced tensor force, V_T and V_C are the tensor force and central force components from H_1 , respectively. The term ΔE_S means the energy denominator is constant for a given n_p, n_h, l_p and l_h set, as discussed above. Here $a = (n_a, l_a, j_a)$, and m_a denotes its magnetic substate, and so on. Note that the two-body states are not antisymmetrized. The states p and h represents particle and hole states, respectively. In the third line of the equation, only particle and hole states are transformed to the ls coupling scheme. Note that the intermediate states are summed up to fulfill spin-saturation within each HO major shell.

We can divide the contribution into two different types according to the spin dependence of the central force. One comes from the terms whose central force part V_C includes $\sigma \cdot \sigma$ (type I) and the other does not (type II). With our summation tailored to a spin-saturated core or an excluded Q -space with all spin-orbit partners, we can prove that type II contributions always vanish because the first factor is diagonal with respect to spin, that is $m_{s_p} = m_{s_h}$, and the second factor is zero when we sum over spin-saturated contributions. Therefore, only a spin-dependent central force results in non-vanishing contributions to the tensor force for higher-order terms in $V_{\text{eff}}^{\text{SM}}$. Finally, the contribution to the tensor force from the spin-dependent central force is quite small because the spin-dependent central force is generally by far smaller than the spin-independent central force in modern realistic NN potentials.

In conclusion, medium effects produce minor contributions to the tensor-force component, resulting in a tensor-force component that is dominated by the bare NN interaction. Our hypothesis about renormalization persistency is fulfilled to a good extent by the tensor force.

Finally, although our analysis has been performed within one major shell only, one should note that this persistency of the tensor-force component via a MBPT renormalization should also hold in the case of multi-shell effective interactions.

VI. TWO-BODY MATRIX ELEMENTS OF THE TENSOR FORCE

In this section we study further renormalization properties of the tensor force by including higher multipole components.

Figure 5 shows the diagonal and off-diagonal matrix elements of the bare tensor force from the AV8' potential, the renormalized $V_{\text{low}k}$ interaction ($\Lambda = 2.1 \text{ fm}^{-1}$) and $V_{\text{eff}}^{\text{SM}}$ obtained by \hat{Q} -box expansion up to the third order with the folded diagram correction, starting from AV8' interaction, similar to what was done in Figs. 2 and 4. From (a) to (d), we display the sd -shell matrix elements, both diagonal (a), (b) and off-diagonal (c), (d) matrix elements. Note that the diagonal matrix elements $\langle j_a j_b | V | j_a j_b \rangle_{JT}$ are specified by the quantum numbers j_a, j_b , and twice the total angular momentum J and total isospin T . Off-diagonal matrix elements $\langle j_a j_b | V | j_c j_d \rangle_{JT}$ are specified by j_a, j_b, j_c, j_d, J and T . The corresponding numbers for the pf -shell are shown in panels (e) through (j). In both the sd -shell and the pf -shell, the patterns are the same as for all the effective interactions and thus the R-Persistency is approximately fulfilled. Especially, for $V_{\text{low}k}$, we can hardly see any difference between the bare tensor force and the tensor force in the effective interaction $V_{\text{low}k}$. For the diagonal matrix elements, we can see small differences between the final \hat{Q} -box and the bare tensor force, however, it does not contradict the results with respect to the monopole component discussed above, mainly because only matrix elements with low angular momentum display sizable differences. Since the monopole terms are weighted by $2J + 1$, matrix elements with larger values of the total angular momentum J carry a much larger weight in Eq. (1). In off-diagonal matrix elements, we see somewhat larger differences. Their role in shell-model calculations needs to be investigated further. A spin-tensor analysis along these lines was made recently by Smirnova *et al* [17].

VII. ANALYSIS OF OTHER INTERACTION MODELS

In the previous sections, we calculated effective interactions starting from the AV8' interaction, using a renormalized interaction and MBPT. We found that the R-Persistence of the tensor force holds for all these renormalization procedures. An obvious question is whether or not the R-Persistence holds for other interaction models as well. In this section we investigate this question.

We employ here another frequently used realistic interaction, $\chi\text{N}^3\text{LO}$, as an example [9]. The $\chi\text{N}^3\text{LO}$ interaction has a relatively smaller coupling between low-momentum and high-momentum modes compared with the AV8' potential. In Fig. 6 we show the monopole part of the tensor force of the $\chi\text{N}^3\text{LO}$ bare potential and $V_{\text{low}k\text{s}}$ with several cutoff parameters $\Lambda(1.0 \text{ fm}^{-1}, 2.1 \text{ fm}^{-1} \text{ and } 5.0 \text{ fm}^{-1})$. These results should be compared with the corresponding ones obtained with the AV8' interaction shown in Fig. 2. Figure 7 shows the tensor-force monopole of $V_{\text{eff}}^{\text{SM}}$, corresponding to Fig. 4 for the AV8' interaction, starting from the $\chi\text{N}^3\text{LO}$ interaction. Finally, Fig. 8 shows the multipole components of effective interactions, corresponding to Fig. 5 for the AV8' interaction.

In all figures, we can conclude that all the features we discussed for the AV8' interaction remain for the $\chi\text{N}^3\text{LO}$ interaction model as well.

VIII. CONCLUSION

In this work we have presented a detailed analysis of various contributions to the nuclear tensor force as function of different renormalization procedures, starting with the state-of-the-art nucleon-nucleon (NN) interactions and ending up with effective interactions for the nuclear shell model. The monopole part of the tensor force is weakly or barely affected by various renormalization procedures, which in our case are represented by a renormalization of the bare interaction and many-body perturbation theory in order to obtain an effective shell-model interaction. This has lead us to introduce the concept of renormalization persistency (R-Persistence) in the study of effective interactions. We studied the

R-persistence of both renormalization procedures and showed via both numerical studies with certain intuitive general explanations and a detailed algebraic analysis of core-polarization terms in perturbation theory, that this is a very robust process. We have also shown that the R-Persistence holds for two-body matrix elements including higher multipole components of the tensor force, although the deviation increases somewhat if multipole components are included in the comparison. We conclude that the two renormalization steps (one for short-range correlation and the other for in-medium effects) do not affect much either the monopole nor the multipole components of the tensor force, apart from slight differences between them. Results starting from two different interactions (AV8' and $\chi\text{N}^3\text{LO}$) leads us to the same conclusion, suggesting that the R-Persistence of the tensor force for low-momentum states is a robust feature. This applies also to other interaction models.

The short-range part of the tensor force enters the renormalization of the central force, in particular in the $T = 0$ channel, producing on average an increased attraction. Since the modification of the tensor force appears to be very minor, the central force carries most of the renormalization effects beyond first order in perturbation theory.

Because the R-Persistence of the tensor force in effective interactions is a robust feature, it may give a simple and concrete starting point for examining and constructing effective interactions, especially phenomenological ones [4]. In particular, since the tensor force plays a significant role in the shell evolution for nuclear systems with either large neutron/proton or proton/neutron ratios, one can extract simple physics messages from complicated many-body systems.

Acknowledgments

We are very grateful to Professors R. Okamoto and H. Feldmeier for valuable discussions. This work is supported in part by Grant-in-Aid for Scientific Research (A) 20244022 and also by Grant-in-Aid for JSPS Fellows (No. 228635), and by the JSPS Core to Core program "International Research Network for Exotic Femto Systems" (EFES).

-
- [1] R. B. Wiringa, V. G. J. Stoks, and R. Schiavilla, *Phys. Rev. C* **51**, 38 (1995).
 - [2] R. B. Wiringa and S. C. Pieper, *Phys. Rev. Lett.* **89**, 182501 (2002).
 - [3] T. Otsuka, T. Suzuki, R. Fujimoto, H. Grawe, and Y. Akaishi, *Phys. Rev. Lett.* **95**, 232502 (2005).
 - [4] T. Otsuka, T. Suzuki, M. Honma, Y. Utsuno, N. Tsunoda, K. Tsukiyama, and M. Hjorth-Jensen, *Phys. Rev. Lett.* **104**, 012501 (2010).
 - [5] S. Bogner, T. T. S. Kuo, L. Coraggio, A. Covello, and N. Itaco, *Phys. Rev. C* **65**, 051301 (2002).
 - [6] S. K. Bogner, T. T. S. Kuo, and A. Schwenk, *Physics Reports* **386**, 1 (2003).
 - [7] T. Kuo and E. Osnes, *Lecture Notes in Physics* **364**, 1 (1990).
 - [8] M. Hjorth-Jensen, T. T. S. Kuo, and E. Osnes, *Physics Reports* **261**, 125 (1995).
 - [9] E. Epelbaum, H.-W. Hammer, and U.-G. Meissner, *Rev. Mod. Phys.* **81**, 1773 (2009).
 - [10] M. W. Kirson, *Physics Letters B* **47**, 110 (1973).

- [11] E. Osnes and D. Strottman, *Phys. Rev. C* **45**, 662 (1992).
- [12] B. Brown, W. A. Richter, R. E. Julies, and B. H. Wildenthal, *Annals of Physics* **182**, 191 (1988).
- [13] A. Nogga, S. K. Bogner, and A. Schwenk, *Phys. Rev. C* **70**, 061002 (2004).
- [14] S. K. Bogner, A. Schwenk, T. T. S. Kuo, and G. E. Brown, arXiv.org **nucl-th** (2001).
- [15] A. Umeya and K. Muto, *Phys. Rev. C* **74**, 034330 (2006).
- [16] R. Tamagaki and W. Watari, *Progress of Theoretical Physics Supplement* **39**, 23 (1967).
- [17] N. A. Smirnova, B. Bally, K. Heyde, F. Nowacki, and K. Sieja, *Physics Letters B* **686**, 109 (2010).
- [18] For the $j = j'$ case, the definition is slightly different.
- [19] A short version of the present results was included in [4], while more substantial, deeper and wider discussions are given in this paper.

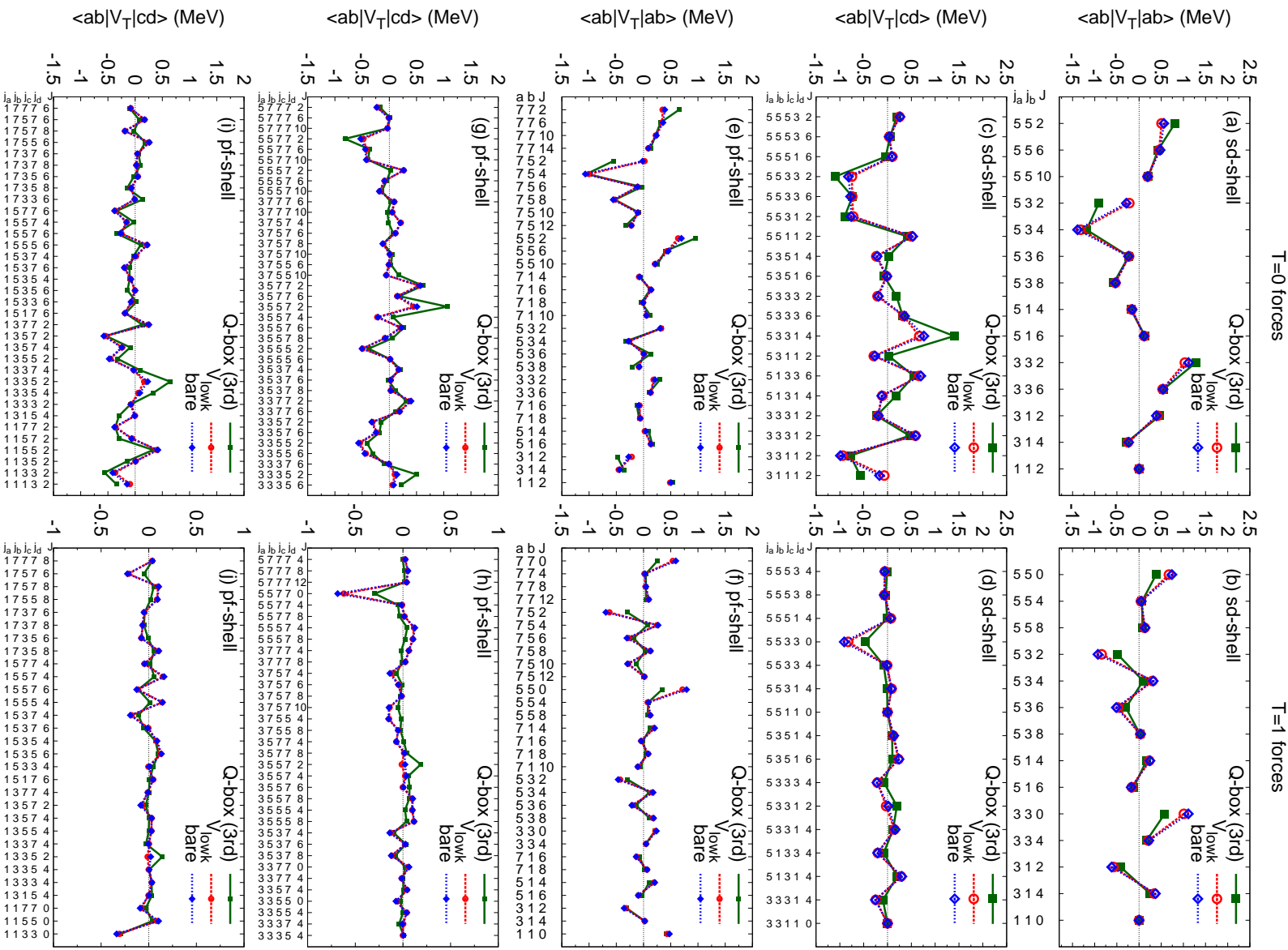


FIG. 5: (color online.) Diagonal and off-diagonal matrix elements of the tensor force component from effective interactions using the AV8' potential.

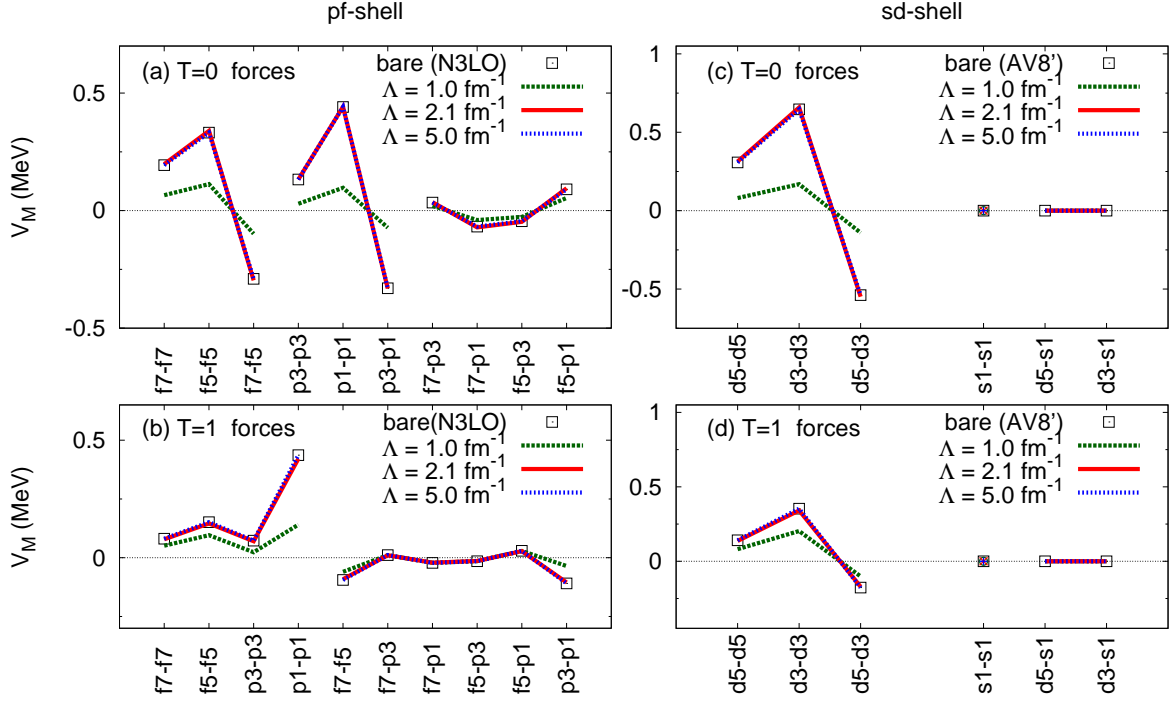


FIG. 6: (color online.) Tensor-force monopole of V_{lowk} starting from the $\chi N^3\text{LO}$ interaction with the same setting as Fig. 2.

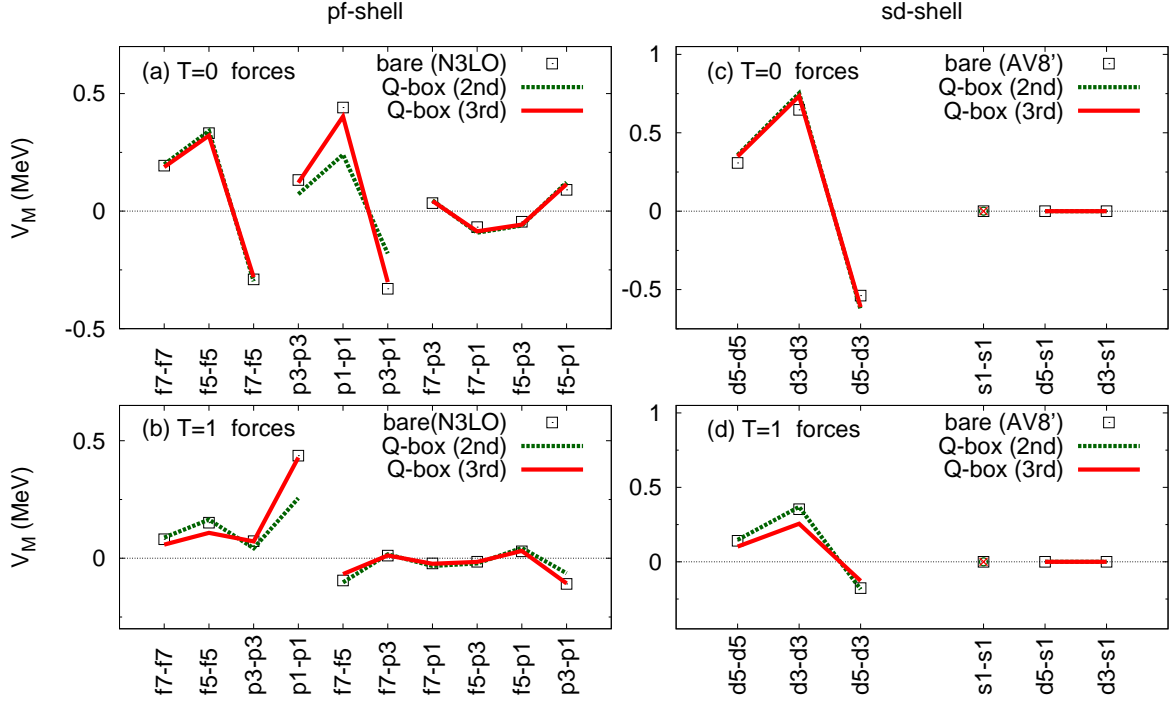


FIG. 7: (color online.) Tensor-force monopole of $V_{\text{eff}}^{\text{SM}}$ starting from the $\chi N^3\text{LO}$ with the same setting as Fig. 4.

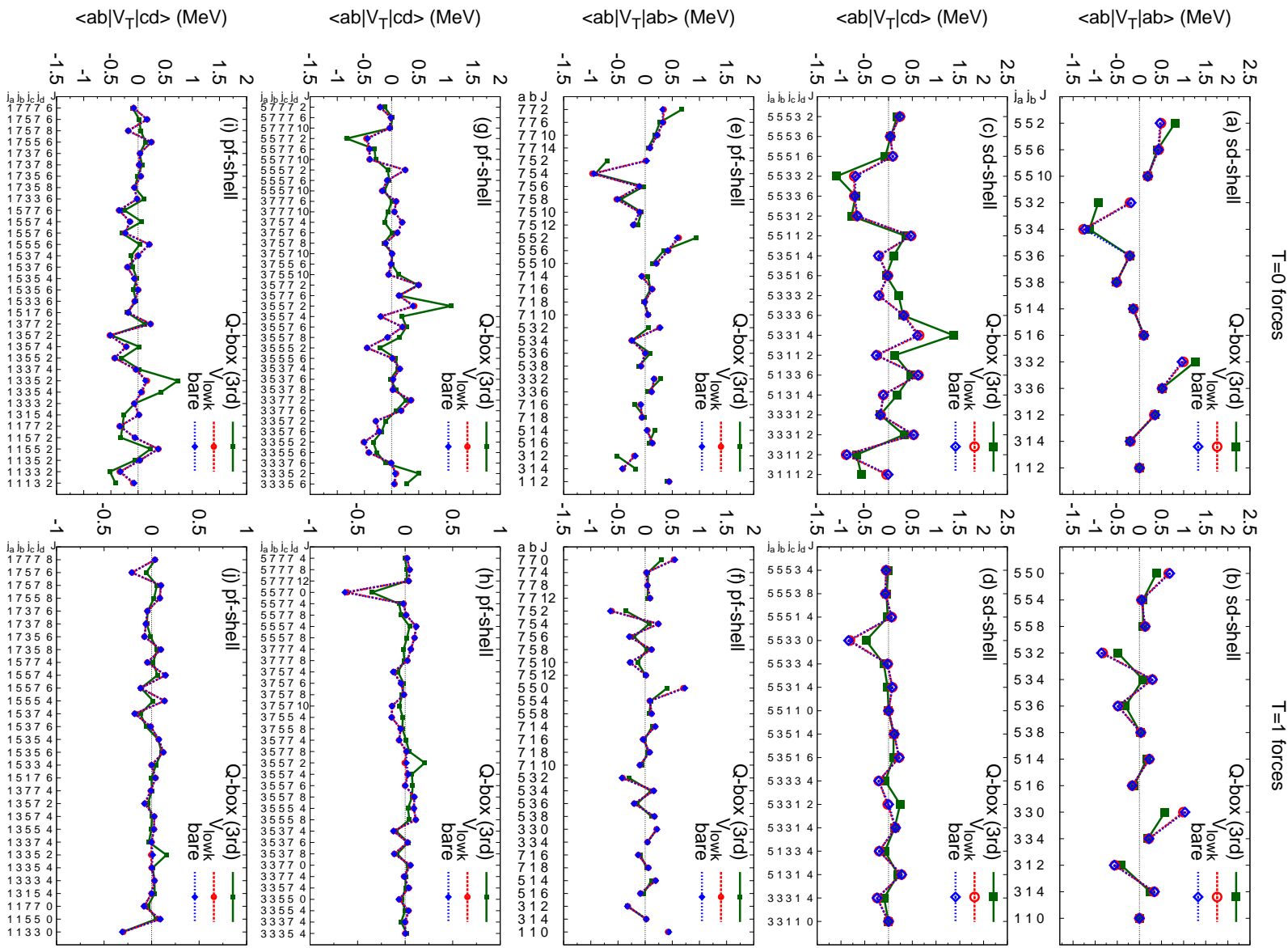


FIG. 8: (color online.) Diagonal and off-diagonal matrix elements of the tensor-force component from effective interactions using the χN^3_{LO} interaction with the same setting as Fig. 5.